



## Reconstructing the exhumation history of the Lesser Himalaya, NW India, from a multitechnique provenance study of the foreland basin Siwalik Group

Yani Najman,<sup>1</sup> Mike Bickle,<sup>2</sup> Eduardo Garzanti,<sup>3</sup> Malcolm Pringle,<sup>4</sup> Dan Barfod,<sup>4</sup> Nick Brozovic,<sup>5</sup> Doug Burbank,<sup>6</sup> and Sergio Ando<sup>3</sup>

Received 28 March 2009; revised 29 June 2009; accepted 29 July 2009; published 30 October 2009.

[1] This research presents the first multitechnique provenance study of the Siwalik Group in the Himalayan foreland basin in India, using the Jawalamukhi section, magnetostratigraphically dated at 13–5 Ma. Combined with provenance data from a Dharamsala Formation sedimentary section (21–13 Ma) located close by, it forms the longest temporally continuous record of Himalayan erosion in the Indian foreland basin. Sandstone petrography and heavy mineral analysis, conglomerate clast composition, Ar-Ar dating of detrital white micas, and Sm-Nd analyses on siltstones, conglomerate matrix and conglomerate clasts was undertaken to determine (1) shifts in source region through time and (2) changes in detrital lag times related to exhumation rates in the hinterland, together interpreted in the light of thrusting events. We interpret the data to show a slow down in exhumation rate of the Higher Himalaya by 16–17 Ma, after which time the locus of thrusting propagated south of the Main Central Thrust, and erosion of the low grade Haimanta Formation to the south became significant. The nonmetamorphosed Inner Lesser Himalaya breached its Haimanta cover by 9 Ma with the metamorphosed Inner Lesser Himalaya (Lesser Himalayan Crystalline Series) exhuming to surface by 6 Ma. This event caused sufficient disruption to established drainage patterns that all Higher Himalayan material was diverted from this location at this time. **Citation:** Najman, Y., M. Bickle, E. Garzanti, M. Pringle, D. Barfod, N. Brozovic, D. Burbank, and S. Ando (2009), Reconstructing the exhumation history of the Lesser Himalaya, NW India, from a multitechnique provenance study of the foreland basin Siwalik Group, *Tectonics*, 28, TC5018, doi:10.1029/2009TC002506.

<sup>1</sup>Lancaster Environment Centre, Lancaster University, Lancaster, UK.

<sup>2</sup>Department of Earth Sciences, Cambridge University, Cambridge, UK.

<sup>3</sup>Dipartimento di Scienze Geologiche e Geotecnologie, Università degli Studi di Milano-Bicocca, Milan, Italy.

<sup>4</sup>SUERC, East Kilbride, UK.

<sup>5</sup>Department of Agricultural and Consumer Economics, University of Illinois, Urbana, USA.

<sup>6</sup>Department of Geological Sciences, University of California, Santa Barbara, California, USA.

### 1. Introduction

[2] The Himalayan orogen provides a type example of continent-continent collision on which a number of models of deformation of the continental lithosphere are based. Tectonic reconstructions are critical to the development of such models. While timing of exhumation of the Higher Himalayan lithotectonic unit is relatively well documented in India [Thiede *et al.*, 2009; Vannay *et al.*, 2004, and references therein] the timing and mechanism by which deformation subsequently propagated south within the thrust belt, to the Lesser Himalayan lithotectonic unit, is considerably less well defined.

[3] This paper examines a sedimentary succession within the Himalayan foreland basin near Jawalamukhi in NW India (Figure 1), dated from 12 to 5 Ma [Brozovic and Burbank, 2000; Meigs *et al.*, 1995]. Combined with the neighboring sedimentary succession dated from 21 to 13 Ma [White *et al.*, 2002] (labeled CMB in Figure 1) this provides the longest record of erosion from the mountain belt preserved in the basin in India. Within this record lies information on the transition of exhumation from the Higher to Lesser Himalaya. Such data will inform theoretical models of crustal deformation by allowing more refined model data comparisons [Jamieson *et al.*, 2004]. In addition, an accurate knowledge of the timing of the exhumation of the Lesser Himalaya is required in order to test hypotheses that relate erosion of this unit to changes in ocean geochemistry [Bickle *et al.*, 2001; English *et al.*, 2000; Galy *et al.*, 1999; Pierson-Wickmann *et al.*, 2000; Quade *et al.*, 1997; Quade *et al.*, 2003].

### 2. Sedimentary Succession

[4] The 12–5 Ma magnetostratigraphically dated Siwalik Group studied here is located in the Kangra reentrant (Figure 1), in the same region as the previously published study of the 21–13 Ma Dharamsala Formation [White *et al.*, 2001]. Both sections are of alluvial facies. The Siwalik section, termed the Jawalamukhi section after a nearby town, is 3400 m thick (Figure 2). As described by Meigs *et al.* [1995] and Brozovic and Burbank [2000], the lower part of the section, from 0 to 470 m, consists of relatively thin (2–5 m in general) sandstone bodies interbedded with siltstones and soil horizons. Between 470 and 1620 m, the succession is dominated by thicker multistoried sandstone bodies (20–30 m thickness in general) with thin conglomeratic beds.

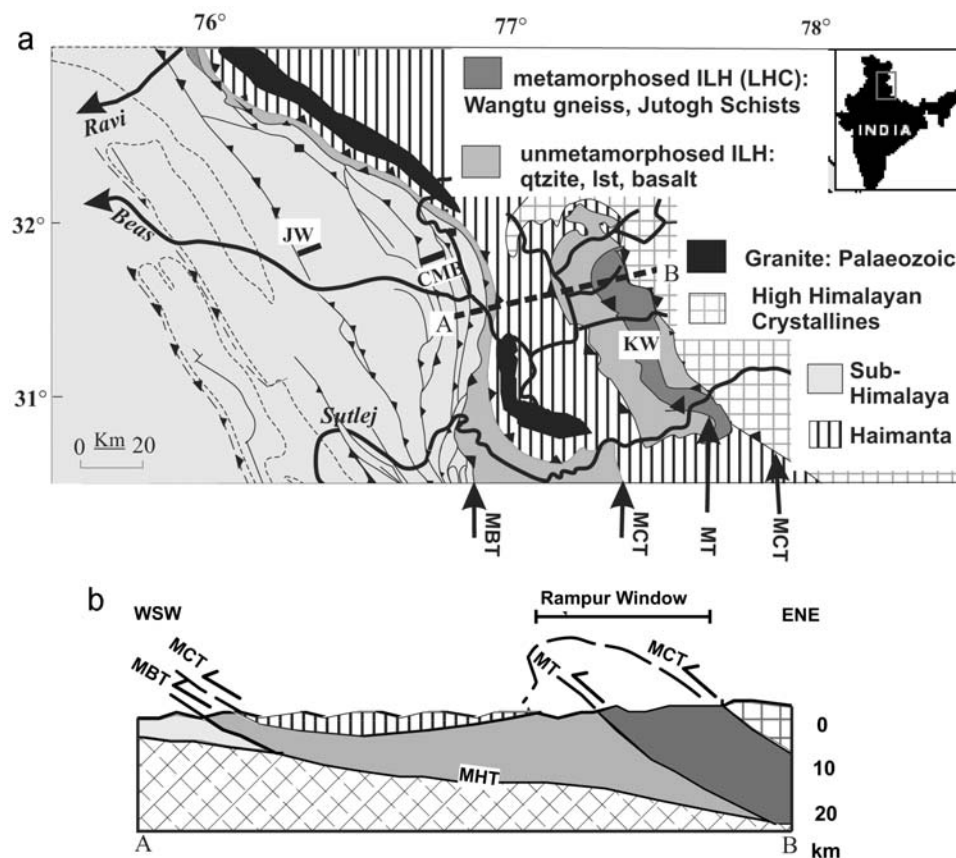


**Figure 1.** (a) Map showing the location of the studied Siwalik section (JW) in the Kangra reentrant, and hinterland geology including the Larji-Kullu-Rampur Window (KW). Map compiled and adapted from Frank *et al.* [1995], Richards *et al.* [2005], Steck [2003], Thiede *et al.* [2004], Vannay *et al.* [2004], and White *et al.* [2001]. Note the position of the Beas River which suggests the direction of the source region. Palaeocurrent data from the Siwalik section indicates that a river system with similar flow direction was in evidence in the past [Brozovic and Burbank, 2000]. Also shown is the location of the Dharamsala Formation studied section located at CMB (CMB, Chimnum-Makreri-Birdhar section) [White *et al.*, 2002]. Dashed line shows approximate location of schematic sketch section (Figure 1b). (b) Sketch section, approximately corresponding to dashed line on map. Not to scale. Adapted from Vannay *et al.* [2004]. ILH, Inner Lesser Himalaya; LHC, Lesser Himalayan Crystalline Series; MCT, Main Central Thrust; JT/MT, Jutogh Thrust/Munsiari Thrust; MBT, Main Boundary Thrust.

From 1620 m to the top of the succession, the lithology is dominated by clast-supported conglomerate. Rare sandstones and siltstones persist, becoming prevalent again in the finer-grained interval between 2100 and 2400 m.

[5] The studied section lies close to the Beas River, a major transverse river which today drains a hinterland which includes the Lesser Himalaya, Rampur Window (also called the Larji-Kullu-Rampur Window (LKRW) in previous studies) and Higher Himalaya to the north (Figure 1). Palaeocurrent indicators from the Jawalamukhi Siwalik section are toward the SW but with variations of WSW, S and, in the lowest part of the section, to the SSE [Brozovic and Burbank, 2000] showing that the rivers which deposited the Siwalik strata drained a similar region to the present-day Beas River. These researchers interpreted the majority of the Jawalamukhi sedimentary section as the deposits of a transverse river, but the basal section (>9 Ma) as deposited

by an axial river. However, our new provenance data suggest that the entire Siwalik sedimentary section at Jawalamukhi was deposited by a transverse river system: By the time of deposition of the basal Siwalik succession, the Higher Himalaya had exhumed rapidly and thus likely dominated the sedimentary signal of any major axial river at the time, as it does today (for example, Ganges River petrography plotted on Figure 3). This is unlike the sedimentary signal seen in the Jawalamukhi section in which Higher Himalayan contribution is subordinate, as detailed in this study.

### 3. Regional Geology of the Hinterland

#### 3.1. Lithotectonic Units

[6] The Himalaya formed when India and Asia collided at ca 55–50 Ma [de Sigoyer *et al.*, 2000; Garzanti *et al.*,

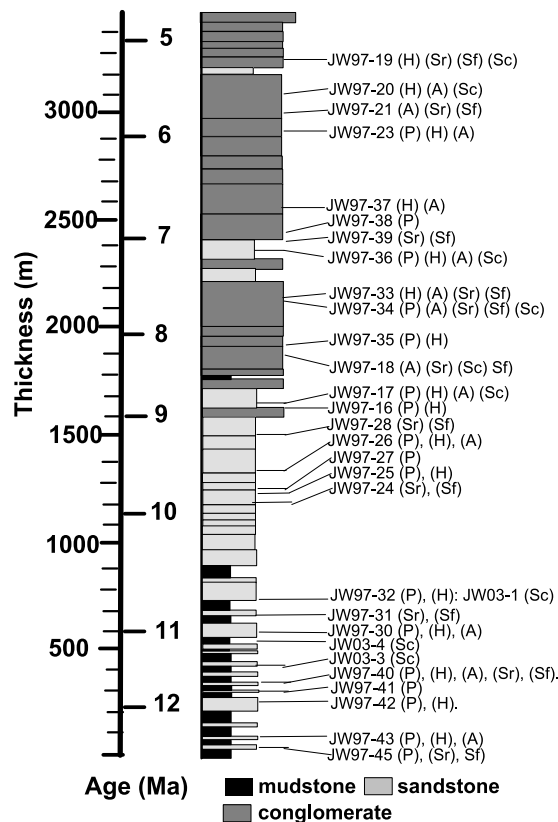


**Figure 2.** Sedimentary section of the Jawalamukhi Siwalik section, with magnetostratigraphy [Meigs *et al.*, 1995] and sample locations marked on. P, petrography; H, heavy minerals; A, Ar-Ar analyses of detrital micas; Sc, Sm-Nd of conglomerate clasts; Sf, Sm-Nd of fine grained facies (conglomerate matrix or siltstone); Sr, Rb-Sr of fine-grained material.

1987; Searle *et al.*, 1997]. South of the suture zone, the Indian crust consists of a number of lithotectonic units, separated by south verging thrusts and a north dipping normal fault (Figure 1). From north to south, the main lithotectonic units are the Tethyan Himalaya, the Higher Himalaya, the Lesser Himalaya and the Sub-Himalaya.

[7] The Tethyan Himalaya consists of Paleozoic-Eocene aged marine sedimentary rocks that were deposited on the northern passive margin of the Indian continent [Gaetani and Garzanti, 1991]. The Tethyan Himalaya is separated from the Higher Himalaya to the south by the South Tibetan Detachment Zone (STDZ). The Higher Himalaya, termed the Higher Himalayan Crystalline Series (HHC), consists of predominantly medium to high-grade rocks metamorphosed in the Cenozoic during the Himalayan orogeny. The unit is overthrust upon the Lesser Himalayan sequence along the Main Central Thrust (MCT).

[8] The Lesser Himalaya in India has been subdivided into the Inner Lesser Himalaya (ILH) and Outer Lesser Himalaya (OLH) on the basis of their differing  $\epsilon_{Nd}$  signatures [Ahmad

*et al.*, 2000; Richards *et al.*, 2005]. The rocks consist predominantly of Precambrian-Paleozoic rocks of varying metamorphic grade. The Outer Lesser Himalaya, which shares a similar  $\epsilon_{Nd}$  signature to the Higher Himalaya (Table 1), is typically of low metamorphic grade, and does not crop out in the region of study. The Inner Lesser Himalaya, which has more negative  $\epsilon_{Nd}$  values than the Higher Himalaya, can be divided into a unit consisting of sedimentary, low grade metamorphic and mafic volcanic rocks, and a unit of medium-high-grade metamorphic rocks termed the Lesser Himalayan Crystalline Series (LHCS). In the region of study, the LHCS is exposed in the Rampur window, separated from the nonmetamorphosed Inner Lesser Himalaya by the Munsiri Thrust (MT). The nonmetamorphosed Inner Lesser Himalaya is also exposed as a narrow strip forming the hanging wall to the Main Boundary Thrust (MBT) to the south. Between this and the Rampur window lies the Haimanta Formation, preserved in a klippe as shown in Figure 1. The Haimanta Formation are considered to be nonmetamorphosed cover to the Higher Himalaya and/or base of the Tethyan Himalaya [Chambers *et al.*, 2009].

[9] The Sub-Himalaya consists of Cenozoic marine and continental sedimentary rocks, eroded from the Himalaya and deposited in the foreland basin to the south of the orogen [Burbank *et al.*, 1996], and is the unit in which the sedimentary succession of this study is located. It is separated from the Lesser Himalaya above by the Main Boundary Thrust and from the present-day foreland basin and Indian craton to the south by the Himalayan Frontal Thrust.

[10] Characteristics of the units of relevance to this provenance study are given in Table 1. The units to the NE of the Jawalamukhi section are the probable source terrain, given the modern day drainage pattern and palaeocurrent indicators (after postdepositional thrusting has been taken into account [Brozovic and Burbank, 2000]). Figure 1 shows this region, the rocks divided broadly into the Higher Himalaya, Inner Lesser Himalaya (nonmetamorphosed and metamorphosed (LHCS) units) and Haimanta Formation, on the basis of lithology, metamorphic grade and isotopic signature.

### 3.2. Tectonic Evolution of the Units in NW India, as Determined From Published Bedrock Data

[11] Following Oligocene tectonic burial [e.g., Vance and Harris, 1999] and metamorphic peak at  $\sim 23$  Ma, rapid exhumation of the Higher Himalaya occurred until  $\sim 19$ – $16$  Ma [Thiede *et al.*, 2009; Vannay *et al.*, 2004]. Exhumation of the Higher Himalaya is thought to have been achieved by extrusion between the MCT below and the Sangla Detachment (part of the STDS) above. Decreased exhumation, interpreted as the result of cessation of movement along the MCT, persisted until  $\sim 3$  Ma, when rapid exhumation resumed [Thiede *et al.*, 2009].

[12] Prograde metamorphism in the Lesser Himalayan Crystalline series of the Rampur Window, due to burial beneath the High Himalaya, was terminated at  $\sim 11$  Ma by tectonic exhumation along the Munsiri/Jutogh Thrust [Caddick *et al.*, 2007; Thiede *et al.*, 2009; Vannay *et al.*, 2004]. Rapid exhumation of the LHCS continued to present-

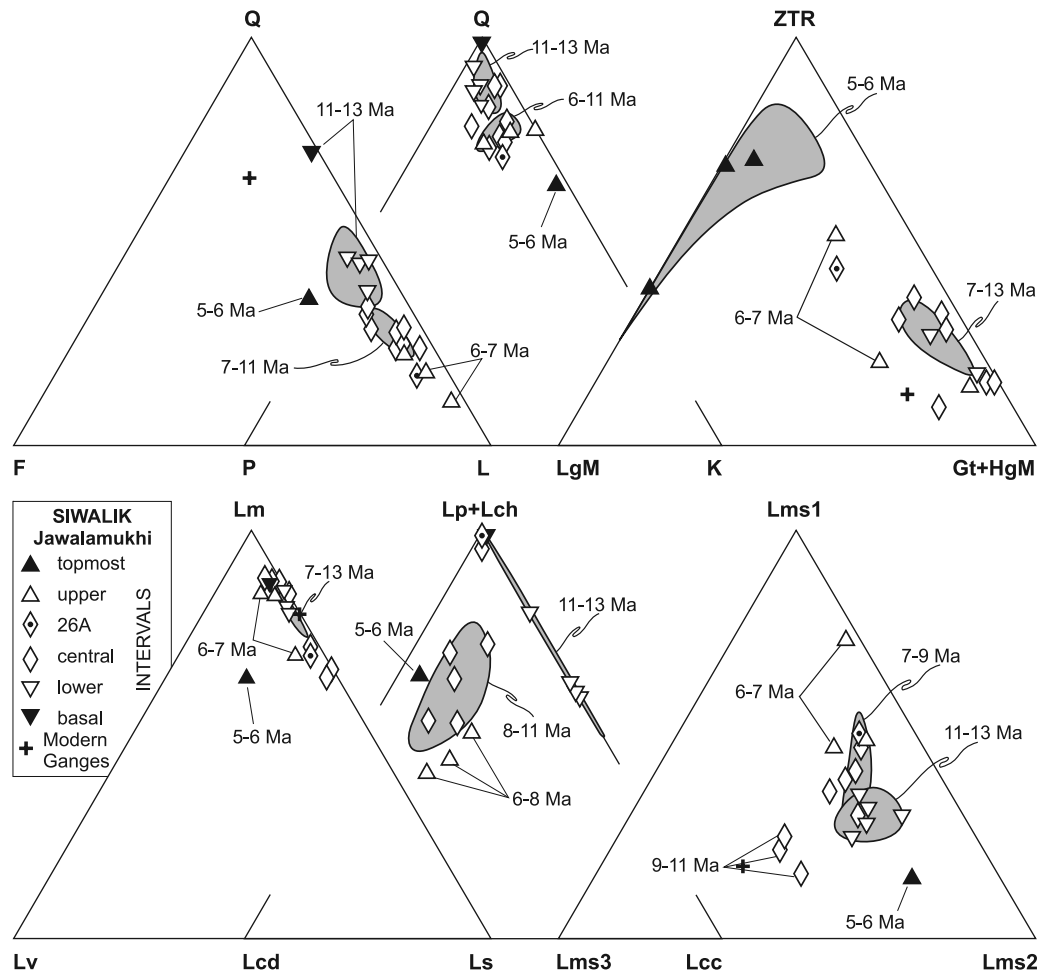


**Figure 3.** Petrography and heavy mineral data. Compositional trends in the Siwalik Jawalamukhi section. Quartzo-lithic to litho-quartzose sandstones of the basal to lower intervals are replaced at  $\approx 11$  Ma by lithic-rich sandstones of the central interval, including abundant dolostone grains after  $\approx 10.5$  Ma. Lithic-dominated sandstones of the upper interval chiefly consist of sedimentary to very low grade metasedimentary detritus, but also include significant basalt after  $\approx 7$  Ma. An abrupt increase in K-feldspar is recorded at  $\approx 6$  Ma, when garnet-dominated assemblages including staurolite, kyanite, and locally sillimanite are replaced by epidotes and ultrastables. Q, total quartz; F, total feldspar (P, plagioclase feldspar; K, K-feldspar); L, total Lithic fragments (Lv, volcanic; Ls, sedimentary; Lp, terrigenous; Lch, chert; Lcc, limestone; Lcd, dolostone; Lm, metamorphic Lms<sub>1</sub>, very low rank slate and metasandstone; Lms<sub>2</sub>, low rank phyllite and quartz/sericite; Lms<sub>3</sub>, medium and high rank schist and gneiss). The 90% confidence regions about the mean are shown. While outliers are plotted, age arrows highlight the mode of values.

day, with Pliocene ( $\sim 5$ – $3$  Ma) to Recent rates either faster [Vannay *et al.*, 2004] or comparable [Thiede *et al.*, 2005, 2009] to rates calculated for the adjacent Higher Himalaya for that period. It has been proposed that the LHCS originally formed the basement to the nonmetamorphosed Lesser Himalayan “cover” rocks beneath the Munsiri Thrust (Rampur and Shali Formations), and was thrust over them in the last few million years [Miller *et al.*, 2000]. Development of the Rampur window may have been associated with the development of ramps along the MBT at the time [Stephenson *et al.*, 2001], which was thought to

have been active by 10–5 Ma [DeCelles *et al.*, 1998; Meigs *et al.*, 1995].

[13] Thus, in summary, the bedrock mineral ages imply that rapid exhumation of the Higher Himalaya between the STDS and MCT slowed down considerably at ca 19–16 Ma when the locus of thrusting transferred south to the Lesser Himalaya. Available bedrock data for the region put peak metamorphism of the LHCS sometime between 11 and 6 Ma according to Vannay *et al.* [2004], with Caddick *et al.* [2007] asserting that exhumation of the Lesser Himalayan Crystalline Series began by 11 Ma. This pulse of rapid exhumation of the LHCS continued until  $\sim 3$  Ma, after

**Table 1.** Characteristics of the Potential Source Lithologies Which May Have Contributed Detritus to the Jawalamukhi Siwalik Section, Documenting Petrographic and Isotopic Signatures Pertinent to This Provenance Study

Lithotectonic Unit	Lithologies	$\epsilon\text{Nd}$ BULK RK	White Mica Ar-Ar Ages
<i>Higher Himalaya (HH)</i> <sup>a</sup> : Mid-Late Proterozoic protolith, Tertiary metamorphic overprint.	Medium-high-grade metamorphic rocks.	$\epsilon\text{Nd}$ (0): -13 to -18 <sup>b</sup>	In vicinity of study area: Bedrock: youngest population ~16 Ma. <sup>a</sup> Beas River draining HH: Youngest grain - 17 Ma, youngest population 18-20 Ma <sup>c</sup>
<i>Inner Lesser Himalaya (ILH)</i> : Early Mid-Proterozoic <sup>b,d</sup> LHCS (Jutogh Group) of ILH	Wangtu orthogneiss (zircon <sup>207</sup> Pb/ <sup>207</sup> Pb age - 1800 Ma <sup>b</sup> , Jutogh mica schists and quartzites Rampur Fm: phyllites, white quartzite, Shali Fm: limestones, dolomites, qtzites. Rampur and Mandi-Darla mafic volcanics. Sedimentary and low grade metamorphic rocks. Greywacke, quartzite, silst, shale, carbonate	$\epsilon\text{Nd}$ (0): -22 to -25 <sup>b</sup>	Bedrock: 7-4 Ma <sup>a,c</sup>
Nonmetamorphosed Fms of ILH. Rampur Fm, Rampur volcanics and Shali Fm found in <i>Rampur window</i> . Shali Fm and Mandi-Darla volcanics found in <i>MBT hanging wall</i> . <i>Haimantia</i> <sup>e,g</sup> : Neoproterozoic		$\epsilon\text{Nd}$ (0): -22 to -25 <sup>b</sup>	No data
<i>Granitoids</i> Cambro-Ordovician granites, e.g., Mandi granite (ca 500 Ma).	Intrude Neoproterozoic units. Exposed as a string directly above MCT, and further north Intrude ILH <sup>b</sup>	$\epsilon\text{Nd}$ (0): (-8) to -19 <sup>b</sup>	No data
Proterozoic granites; 1800-1900 Ma		$\epsilon\text{Nd}$ (500): -9 to -10 <sup>b</sup>	
		$\epsilon\text{Nd}$ (1840): -6.2 <sup>i</sup>	

<sup>a</sup>Yannay et al. [2004].

<sup>b</sup>Richards et al. [2005].

<sup>c</sup>This study.

<sup>d</sup>In the Rampur Window, the Munsiri Thrust separates medium-grade metamorphosed Lesser Himalaya Crystalline Series (LHCS) from low/nonmetamorphosed formations. Nonmetamorphosed Fms are also found in MBT hanging wall.

<sup>e</sup>Thiede et al. [2005].

<sup>f</sup>Frank et al. [1995].

<sup>g</sup>Steck [2003].

<sup>h</sup>Miller et al. [2001].

<sup>i</sup>Miller et al. [2000].

which time exhumation proceeded at comparable rates to the Higher Himalaya [Thiede *et al.*, 2005, 2009].

## 4. Petrographic and Isotopic Analyses on the Siwalik Jawalamukhi Section Detrital Material

### 4.1. Lithologies of the Eroded Detritus

#### 4.1.1. Sandstone Petrography and Heavy Mineral Analyses

[14] The sandstone petrography and heavy mineral analyses are shown in Figures 3 and 4 and Table S1. Three hundred grains from each of 18 thin sections from the Siwalik Group of the Jawalamukhi section were point counted using the Gazzi-Dickinson method [Ingersoll *et al.*, 1984; Zuffa, 1985], and 200 to 250 transparent dense minerals were counted from each of 16 samples by the “ribbon-counting” or “Flett” methods [Mange and Maurer, 1992] (results summarized in Tables S1a and S1b).<sup>1</sup>

[15] The rocks are quartzo-lithic to lithic sandstones, derived predominantly from sedimentary and very low grade metasedimentary sources, as evidenced by the grade of the lithic fragments. Detrital quartz is prevalent at the base of the section, decreasing markedly upsection, indicative of recycling from older sedimentary rocks. Sedimentary lithic fragments include sandstones, argillites, chert and carbonate, the latter showing a dominance of dolomite since 10.6 Ma. Volcanic lithic fragments are negligible in the lower part of the succession. Mafic volcanic and granitoid/orthogneiss rock fragments and conglomerate clasts appear above the start of the conglomeratic facies at 9 Ma. This is a harbinger for the major increase in basalt and granitoid lithic fragments (also seen in the clast count proportions), dolostone and quartzite seen at 6 Ma. Coeval with this event at 6 Ma, the subordinate higher grade metamorphic contribution was entirely cut out, as illustrated by the drastic reduction in garnet. Prior to 6 Ma, higher grade metamorphic material contributed to the detritus in minor quantities. Progressive exhumation of higher grade metamorphic rock is documented by increasing abundance of higher grade metamorphic minerals upsection: garnet, staurolite, and rare kyanite are present from the base of the section, with kyanite becoming more common and sillimanite first appearing at ca. 9 Ma.

#### 4.1.2. Conglomerates

[16] The thick conglomeratic facies extends from 9 Ma to top of the section (5 Ma) in the sedimentary record at Jawalamukhi, with thin conglomeratic beds interbedded with sandstones, down to 11 Ma. 100 conglomerate clasts, >1 cm in diameter, were taken from each of 10 stations, spanning both the thin conglomerate units >9 Ma, and the extensive conglomerates <9 Ma. In Figure 5 the clasts are assigned to one of five categories: granitoid-gneiss, mafic igneous, quartzite, clastic sedimentary clasts excluding quartzite, and carbonate. Distinguishing between a mafic igneous composition and a sandstone proved difficult for a very fine grained, very dark gray clast type. These clasts have been assigned to the nonquartzite clastic

sedimentary category in Figure 5. Only those clasts clearly identifiable as mafic igneous by the presence of acicular crystals, phenocrysts, or other clearly identifiable igneous textures, are assigned to the mafic igneous category in Figure 5.

[17] Most clasts were subrounded to well-rounded. A number of clasts >10 cm diameter occur (largest, 21 cm), with modes (excluding clasts <1 cm diameter) consistently between 3 and 5 cm diameter. Trends in proportions of the various lithological categories are seen: Granitoid-gneiss is rare before 9 Ma, showing a significant increase thereafter. Mafic igneous clasts are rare, becoming more common after 6 Ma. Purple quartzite (not shown as a separate category in Figure 5) is present from the base of the conglomeratic unit but shows a major increase after 6 Ma. The nonquartzite clastic sedimentary clasts show a variety of lithologies, including sandstones and siltstones of varying color, grain size and hardness. A good variety of all such sedimentary clasts types are represented at all stations, except above 6 Ma, represented by Station JW03–15 where only a few purple sandstones are present, and Station JW03–7 where the only sedimentary clasts recorded consist of the very dark gray, very fine grained sedimentary/igneous rock of indistinct provenance, as described above.

### 4.2. Sr-Nd Analyses of Bulk Rock and Conglomerate Clasts

[18] Five conglomerate matrix samples, two of which were subdivided into fine and coarse fractions, and eight mudstones/siltstone samples were analyzed for Sm-Nd and Rb-Sr isotopic compositions. In addition, 12 clasts of varying lithologies, taken from conglomerate beds located above 1620 m (9 Ma) in the section, and 10 small pebbles which occur infrequently in the sandstones between 750 and 393 m (10.6–11.3 Ma), were analyzed for Sm-Nd isotopic compositions. No pebbles were found in the basal part of the section. Dissolution and analytical methods for Sr and Sm-Nd isotopic analyses are as in the work by White *et al.* [2002] except that Rb and Sr concentrations were measured by isotope dilution on a Nu MC-ICPMS with Sr isotopic fractionations corrected and normalized during the analysis to  $^{86}\text{Sr}/^{88}\text{Sr} = 0.1194$  and Rb isotopic composition normalized by sample standard bracketing assuming a power law fractionation factor. The Rb/Sr ratios are accurate to better than  $\pm 1\%$ . Nd blanks were less than 250 pg and Sm blanks less than 120 pg. Analyses of the Cambridge JM Nd standard gave  $^{143}\text{Nd}/^{144}\text{Nd} = 0.511121 \pm 18$  ( $2\sigma$ ) and analyses of the NBS987 standard gave  $0.710250 \pm 18$  ( $2\sigma$ ) during the period of the analyses.

[19] The results are summarized in Table S2 and Figure 6. Bulk rock  $\epsilon_{\text{Nd}}(0)$  values for both conglomerate matrix and siltstone remain constant from the base of the section until 6 Ma, with an average value of  $-15$ , marginally more negative for the conglomerate matrix. After 6 Ma, values become distinctly more negative, at  $-18$  to  $-19$  for siltstone and  $-23$  for conglomerate matrix.  $\epsilon_{\text{Nd}}(0)$  values for conglomerate clasts show no clearly defined temporal trend. Clasts with distinctly negative  $\epsilon_{\text{Nd}}(0)$  values ( $\sim -25$ ) occur from 9 Ma onwards.

<sup>1</sup>Auxiliary material data sets are available at <ftp://ftp.agu.org/apend/tc/2009tc002506>. Other auxiliary material files are in the HTML.

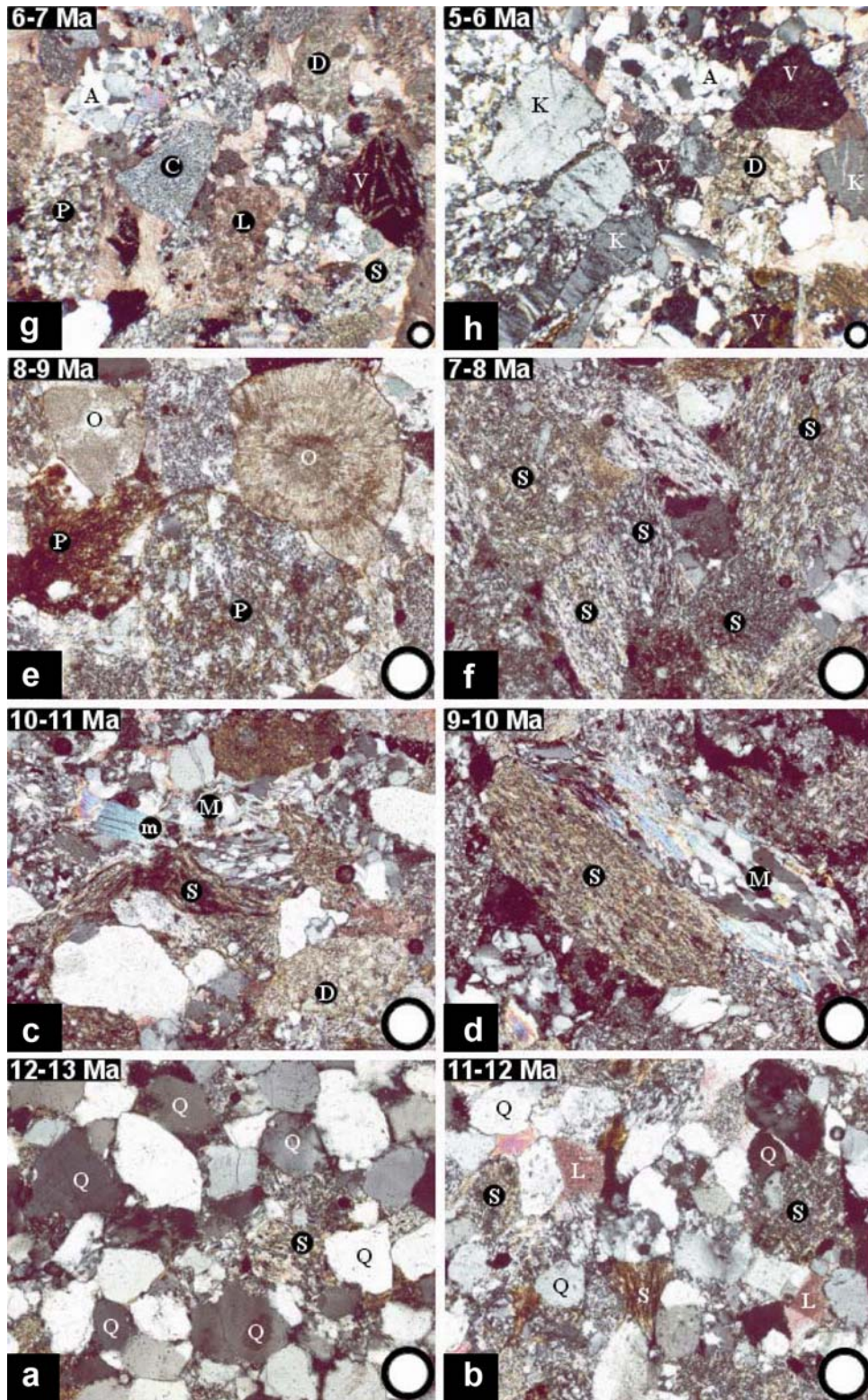
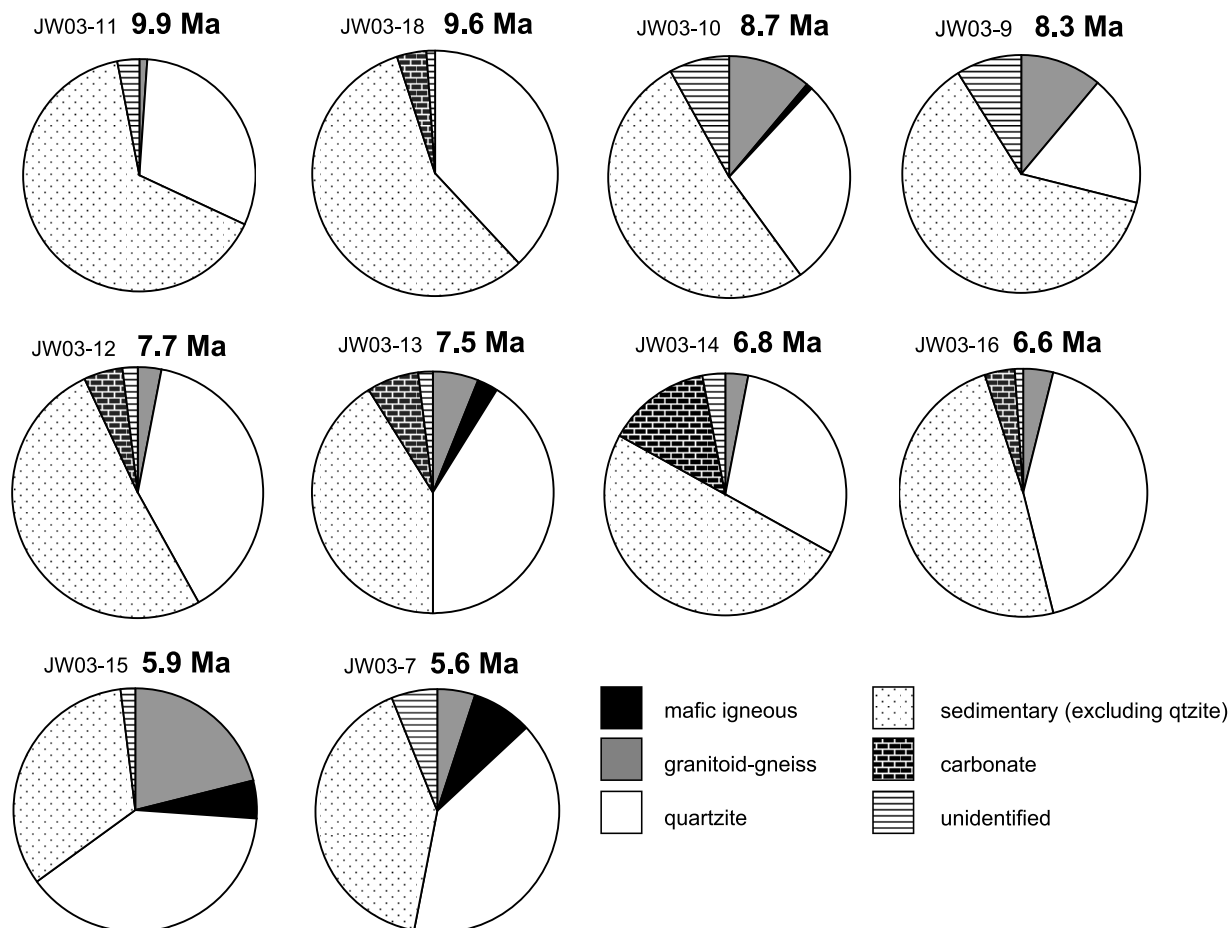


Figure 4



**Figure 5.** Conglomerate clast counts (100 clasts counted, of diameter >1 cm, at each station). The category “mafic igneous” only includes those clasts clearly identifiable as such in the field, by the appearance of distinctive igneous texture. The origin of one clast type (igneous or sedimentary), a very fine grained, dark gray rock, was difficult to determine in the field and was assigned to the “sedimentary” category. The “unidentified” category contained unrecognizable clasts, mainly due to heavy weathering or alteration.

#### 4.3. Ar-Ar Analyses of Detrital White Micas

[20] Between 20 and 35 grains from each of 15 Siwalik samples from the Jawalamukhi section were analyzed by total fusion, following the method as described by *Najman et al.* [2003]. In addition, a further Siwalik sample (JK99-01), magnetostratigraphically dated at 5–6 Ma, from Haripur, outside the Kangra reentrant [*Sangode et al.*, 1996] was analyzed. Modern river sands were collected from the Beas River, a major transverse river which drains

the Higher Himalaya. A sample was collected where the river enters the Sub-Himalaya at Mandi, and to the north at Kullu, upstream of the Rampur Window. Results are shown in Figures 7 and 8, and tabulated in Table S3.

[21] From the base of the Jawalamukhi section until 7.7 Ma, Cenozoic aged micas dominate the mica population in most samples, with subordinate populations stretching to the Cambrian. The youngest grain in each sample lies between 15 and 18 Ma and the youngest modes between 16

**Figure 4.** Changes in bulk petrography recorded through the Jawalamukhi Siwalik section. (a and b) Sedimentary to very low grade metasedimentary Indian margin units provide the bulk of the detritus. (c and d) Greatest abundance in higher-rank metamorphic rock fragments and detrital feldspars indicate increasing detritus from medium-high-grade rocks between 10 and 11 and 9–10 Ma. Dominance of dolomite over limestone first occurs. (e and f) Detrital modes document dominant very low grade to sedimentary sources upsection. (g and h) Appearance of lathwork volcanic grains (upper interval; 6–7 Ma) heralds a prominent change to detritus dominated by K-feldspars and granitoid/orthogneiss rock fragments (topmost interval; 5–6 Ma) Main grain types: Q, quartz; K, K-feldspar; V, mafic volcanic; O, oospirite; L, micritic limestone; D, dolostone; A, sandstone; P, siltstone/shale; C, chert; S, slate; M, micaschist; m, muscovite. All photos with crossed polars; white dot is 125  $\mu\text{m}$  in diameter.

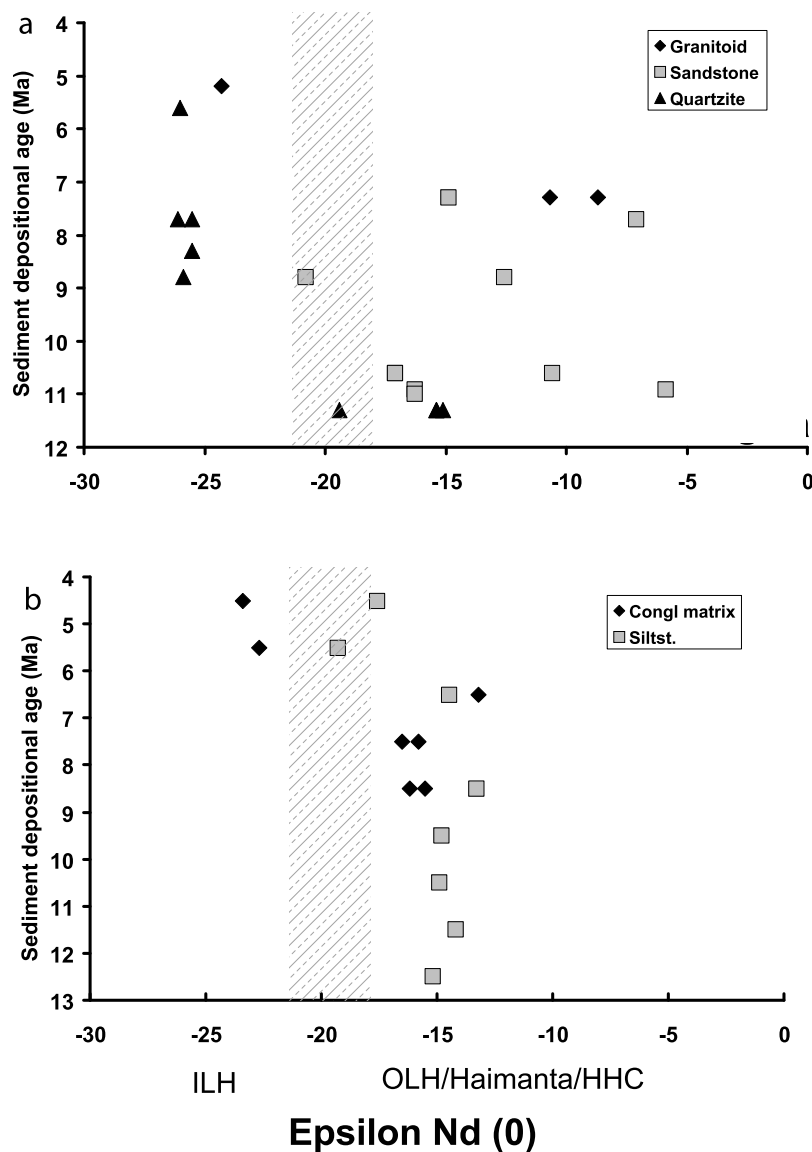
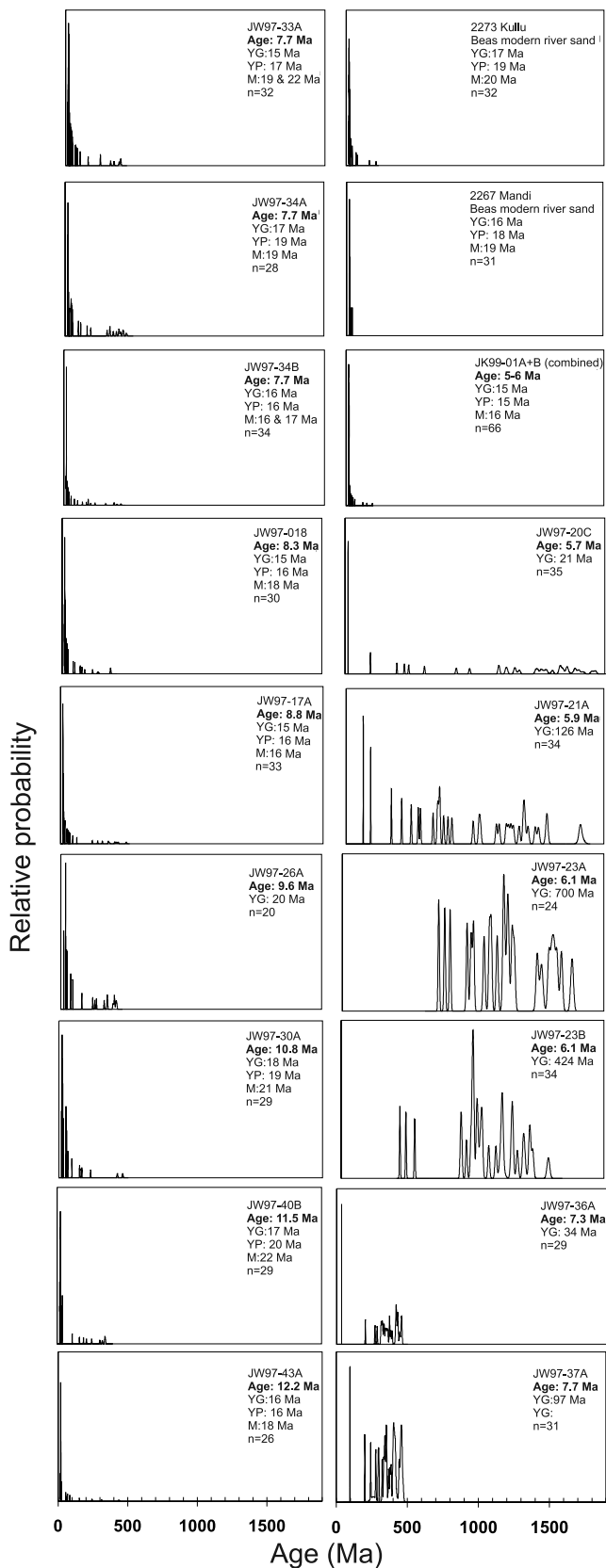


**Figure 6.** (a) The  $\epsilon_{Nd}$  whole rock data for conglomerate clasts and (b) bulk rock conglomerate matrix and siltstone. Hatched gray zone represents demarcation between Inner Lesser Himalaya (ILH) and Higher Himalayan Crystallines (HHC), Haimanta and Outer Lesser Himalaya (OLH) taken from *France-Lanord et al.* [1993, and references therein] and *Richards et al.* [2005], recalculated to  $\epsilon_{Nd}(0)$ .

to 22 Ma. Between 7 to 6 Ma, Cenozoic grains are almost entirely absent, with the mica population dominated by Paleozoic and Mesozoic grains. At 6 Ma another change occurs, and the Palaeozoic-Mesozoic grains become subordinate to Proterozoic grains. The continuing prevalence of Cenozoic mica populations in sample JK99–01 located outside the reentrant in Haripur, and dated between 5 and 6 Ma, indicates that these changes are local, not basin wide.

[22] Lag times (the difference between the mica Ar-Ar age and the host sediment depositional age, an indicator of exhumation rate of the source region [*Bernet et al.*, 2001]) range between 4.1 and 10.4 Myr as calculated for youngest grains, and 5.8–11.3 Myr as calculated for modes (Figure 9). Seven samples, which lacked Cenozoic populations (no

Cenozoic aged grains or one grain only), are excluded from the plot. In some instances our data set shows considerable variation in youngest grains and modes for coeval samples, possibly the result of the relatively small number of grains analyzed per sample [e.g., see *Amidon et al.*, 2005]. Combining data from samples of near coeval age to improve the analysis number was therefore also undertaken to better understand the consequences of small sample size on our interpretations: data from three samples ranging in depositional age from 10.8 to 12.2 Ma were amalgamated, as were data from four samples aged between 7.7 and 8.8 Ma. Comparison with data from single samples of similar age show that the mode is lowered by 2–4 Myr, bringing it closer to the youngest grain age. When combined with data



from the older Dharamsala Formation record of *White et al.* [2002] located close by (Figure 1), Figure 9 shows a clear change in lag time at 17 Ma, from <1 Myr prior to 17 Ma, to between 5 and 10 Myr after 17 Ma, except for samples between ~12 and 11 Ma. After 17 Ma the lag times are broadly consistent with ‘steady state exhumation’ at rates between 1 and 2 mm/a (calculated as by *White et al.* [2002]).

## 5. Interpretations

### 5.1. Provenance of the Jawalamukhi Siwalik Sedimentary Rocks

[23] Mafic igneous detritus (occurring as both lithic fragments in sandstones, and as conglomerate clasts) is most likely derived from the nonmetamorphosed Lesser Himalaya, e.g., the Rampur volcanics of the Rampur Window or Mandi-Darla volcanics in the hanging wall of the MBT. Potential sources for the granitoid-gneiss detritus could be the Higher Himalaya, Haimanta or Lesser Himalaya (LHCS). Potential sources for the sedimentary lithic detritus include the Haimanta Formation, Lesser Himalaya, or recycled earlier foreland basin deposits. The Sm-Nd data from the conglomerate clasts (Figure 5) permits provenance discrimination between these alternative potential sources, as described below.

[24] The bulk rock  $\epsilon_{Nd}$  values indicate that the bulk of the fine-grained sediment was derived predominantly from Higher Himalaya or Haimanta until 6 Ma (Table 1). However, analyses of clasts show that a proportion of the sediment was derived from the Inner Lesser Himalaya from at least 9 Ma. Clasts identified as Inner Lesser Himalayan on the basis of their  $\epsilon_{Nd}$  values include quartzites and a foliated granitoid (clast JW97-19B CT1, depositional age 5.2 Ma) that has an  $\epsilon_{Nd}$  (1800) value similar to that of Proterozoic granitoids in the Rampur Window [Miller *et al.*, 2000]. Nonquartzite sedimentary clasts have  $\epsilon_{Nd}$  values consistent with derivation from the Haimanta Formation and some quartzite clasts also have Haimanta signature. Granitoid clast sample JW97-36B CT1, (depositional age 7.3 Ma) has an  $\epsilon_{Nd}$ (500) value similar to the Palaeozoic granites (e.g., the Mandi granite [Miller *et al.*, 2001]) which intrude these Haimanta rocks.

[25] The white micas with Cenozoic Ar-Ar ages, which are dominant in sandstone samples aged >7.7 Ma, were in all probability derived from the Higher Himalaya. Both their modes and youngest grain ages compare well with ages of

**Figure 7.** Probability density plots of Ar-Ar ages of white mica grains for modern river sands (2273 Beas River at Kullu; 2267 Beas River at Mandi), Siwalik sandstone from Haripur section outside the Kangra reentrant (JK99-01A and JK99-01B), and Siwalik samples from the Jawalamukhi section (JW). Age is magnetostratigraphically determined depositional age of the sample, and n is number of analyses. YG, youngest grain age; YP, youngest age from more than one grain; M, mode. YP and M only given where sample contains more than one Neogene aged grain.

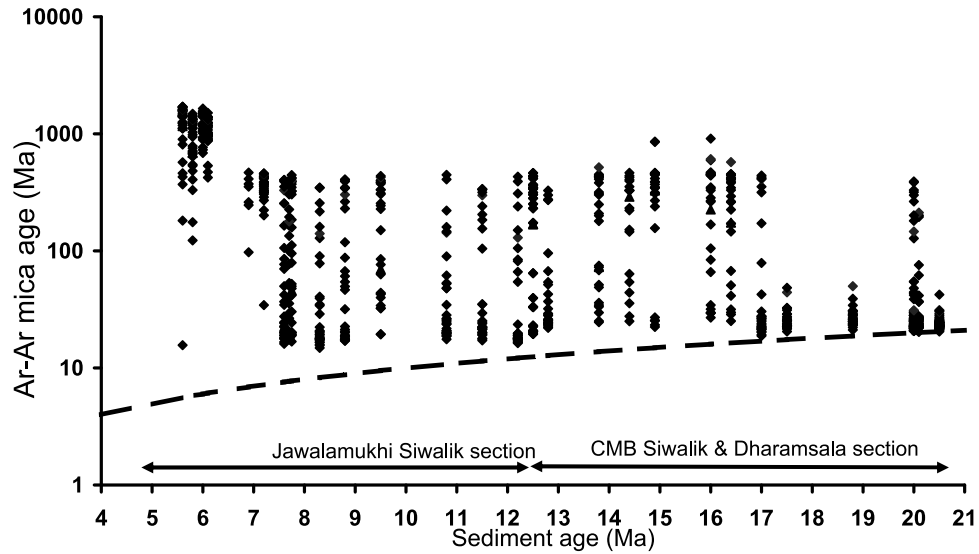


**Figure 8.** Ar-Ar ages of white micas, including previously published data from the Dharamsala and lowest Siwalik rocks of the Chimnum-Makreri-Birdhar section (CMB) [White *et al.*, 2002] (Figure 1) as well as our new data from the Siwalik Group at Jawalamukhi (JW), showing short lag times until 16 Ma, and a major change of provenance at 6–7 Ma. Dashed line on graph is 1:1 line, where mica age equals depositional age. Grains falling on this line have zero lag time.

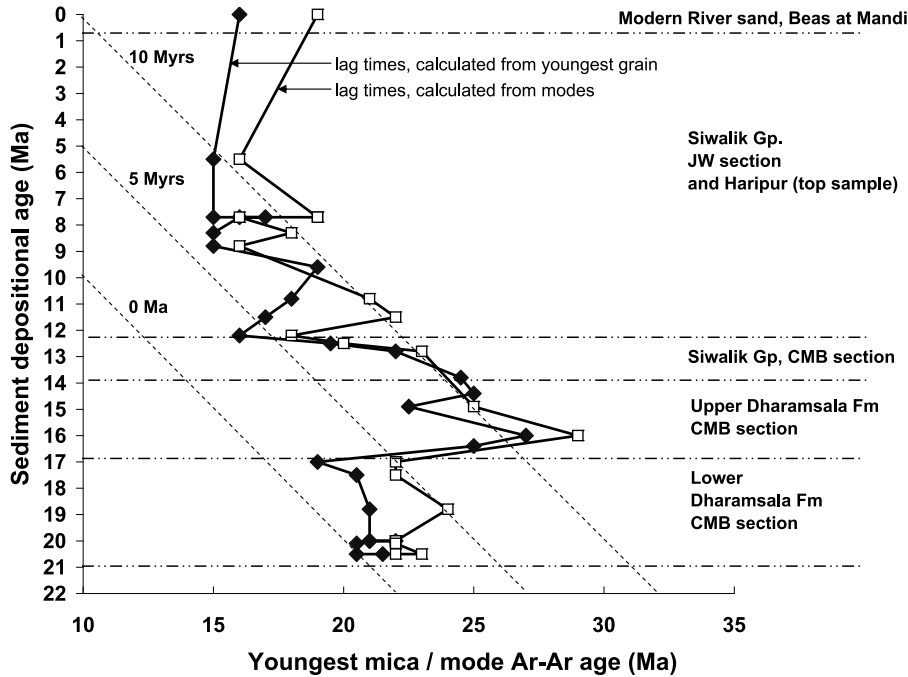


**Figure 9.** Ar-Ar mica ages of youngest grain and youngest mode in each sample, plotted to show exhumational state of the Higher Himalaya over the time period 21–0 Ma, determined from the variation in lag times up section. Dashed lines are times of equal lag time of 0 Myr, 5 Myr, and 10 Myr lag time as labeled. Points which fall near 0 Myr lag time indicate a period of rapid exhumation. Lag time trends which lie parallel to a dashed line indicate a period of steady state exhumation. Trends which cross lines indicate departure from steady state, to either increasing exhumation rates (decreasing lag times up section) or decreasing exhumation rates (increasing lag times up section). Line with diamonds indicates lag times calculated using youngest grain, and line with squares indicates lag times calculated using youngest mode.

micas from Higher Himalayan bedrock and from detrital grains from the Beas River (Table 1). The Lower Palaeozoic grains which are also present in these samples, and dominant in the samples dated between 6 and 7 Ma are likely derived from the Cambro-Ordovician granites intruding Haimanta/Higher Himalayan lithologies. The Proterozoic grains, which dominate the mica populations in samples <6 Ma, are likely derived from Proterozoic granitoids such as the Wangu gneiss, which intrude the Lesser Himalayan Crystalline Series.

## 5.2. Tectonic History of the Hinterland, as Determined From the Siwalik Detrital Record

[26] In the Siwalik rocks of the Jawalamukhi section, the dearth of mica Ar-Ar ages younger than 16 Ma suggests that, in this region, rapid exhumation of the Higher Himalaya had ceased by this time. This lack of mineral ages younger than 16 Ma is in agreement with mica ages determined from bedrock studies of the area [Thiede *et al.*, 2005; Vannay *et al.*, 2004] and our new ages of detrital micas taken from modern river sands draining the Higher Himalaya in this region (samples 22267 Mandi and 2273 Kullu). Slow down of exhumation before 16 Ma is consistent with the cooling curve constructed for the Higher Himalaya of the region [Thiede *et al.*, 2009; Vannay *et al.*, 2004] and with an increase in lag time between sediment depositional age and Ar-Ar ages of Higher Himalayan sourced detrital white micas at 17 Ma, as determined from the Dharamsala Formation section [White *et al.*, 2002] (Figures 8 and 9).

[27] This time of slowdown of exhumation of the Higher Himalaya is proposed to represent the period when thrusting propagated southwards into the footwall of the MCT [Caddick *et al.*, 2007; Chambers *et al.*, 2009; Vannay *et al.*, 2004], with the Higher Himalaya continuing to exhume more slowly after this time, burying the Lesser Himalayan Crystalline Series metamorphosed at ~11 Ma. This protracted slower exhumation of the Higher Himalaya is verified by the detrital record. Broadly, lag times remain constant up section, 6–7 Myr (calculated from youngest grain) over the time interval 16 to 7 Ma, thus describing a moving peak defining (on a coarse temporal scale) steady state exhumation of the Higher Himalaya over this time period, but at a slower rate than prior to 17 Ma. The abrupt increase in lag time at 17 Ma is accompanied by a switch in provenance from predominantly metamorphic detritus of Higher Himalayan source, to predominantly sedimentary/very low grade metamorphic detritus, interpreted as eroded from the Haimanta Formation [White *et al.*, 2002] lying to the south of the Higher Himalaya and indicative of southward propagation of thrusting. The excursion to higher exhumation rates between 12 and 11 Ma and possibly to 8 Ma is consistent with the higher exhumation rate (2 to 3 mm/yr) of the relatively thin crustal segment between the MCT and Munsiri Thrust inferred by Caddick *et al.* [2007] from the P-T-t evolution of one LHCS sample.

[28] Initial input of Inner Lesser Himalayan material into the detrital record, when the Rampur Window breached its Haimanta cover, is difficult to detect using the techniques we employed. This is because the low grade metamorphic

and sedimentary lithic fragments may be sourced either from the Lesser Himalaya or the Haimanta Formation, many Lesser Himalayan lithologies are mica-poor, and the more negative Lesser Himalayan  $\epsilon_{\text{Nd}}$  signal is swamped in bulk rock analyses by dilution with Haimanta/Higher Himalayan detritus which continued to contribute significant amounts of detritus to the basin, as evidenced by the prevalence of Cenozoic micas and bulk rock  $\epsilon_{\text{Nd}}$  values with Haimanta/Higher Himalayan signature.

[29] Sm-Nd analysis on pebbles, which are present in the sedimentary record from 11 Ma onward, overcomes the problem of signal swamping by Haimanta/Higher Himalayan dilution in bulk rock analyses. In the lower part of the succession, below the onset of thick conglomerate beds at 1680 m (8.8 Ma) all of the pebbles analyzed have  $\epsilon_{\text{Nd}}$  values typical of Haimanta/Higher Himalaya affinity, with their sedimentary lithologies confirming Haimanta rather than Higher Himalayan provenance. The first Inner Lesser Himalayan clast (of sedimentary lithology) was detected at 1680 m within the succession (8.8 Ma). The nonmetamorphosed Inner Lesser Himalaya was thus exhumed to surface by this time, consistent with bedrock data [Caddick *et al.*, 2007; Vannay *et al.*, 2004]. However, initial erosion of this unit may have occurred earlier but its detritus may lie undetected in the sedimentary record: Clasts in the older part of the succession, to 11.3 Ma, are very rare, and sampling may have missed a Lesser Himalayan derived pebble. Prior to 11.3 Ma no clasts were found and a small Lesser Himalayan input would go undetected in the sandstone and mudstone fractions, using the techniques described. Possible evidence for initiation of Lesser Himalayan erosion by 10.6 Ma may be the dominance of dolomite over limestone, typical of the Lesser Himalaya, as lithic fragments in sandstones, at this time. From 9 Ma, the conglomeratic facies, with clasts of mixed Haimanta and Lesser Himalayan lithologies attest to the prevalence of a proximal source. Lesser Himalayan clasts are of sedimentary origin, indicating that it is nonmetamorphosed Inner Lesser Himalayan “cover” rather than the metamorphosed Inner Lesser Himalaya (LHCS) that was being exhumed during that time, consistent with the common occurrence of mafic volcanic lithic fragments recorded.

[30] Beginning at 7 Ma, Higher Himalayan material is cut out in the Jawalamukhi section and detritus was entirely derived from more proximal sources in the Lesser Himalaya. We interpret this drastic change as the result of trunk (Higher Himalaya draining) river diversion away from the section of study due to thrust tectonics as the metamorphosed Inner Lesser Himalaya (LHCS) breached surface: Between 7 and 6 Ma, Higher Himalayan Cenozoic aged white micas are cut out; Sm-Nd bulk rock values; dominance of Palaeozoic white micas likely derived from Cambro-Ordovician granites; and the presence of a granitoid clast of such an affinity (JW97–36B CT1 and CT2, depositional age 7.3 Ma) attest to continued substantial input from the Haimanta. At 6 Ma, garnet (presumably Higher Himalayan derived) is cut out and increased erosion from the nonmetamorphosed Inner Lesser Himalayan “cover” is signaled by the major influx of mafic volcanics and dolomite lithic fragments. Palaeozoic

white micas are drastically reduced, replaced by a flood of Proterozoic grains derived from Proterozoic granitoid gneisses intruding the Lesser Himalaya, such as the Wangu gneiss of the Lesser Himalayan crystallines series. A granitoid conglomerate clast of such affinity (JW97–19B CT1, depositional age 5.2 Ma) confirms erosion of the LHCS by this time, coincident with a major increase in granitoid lithic fragments as documented from sandstone petrography. Such material heralds the earliest observed record of erosion of the metamorphosed LHCS, such as that exposed in the Rampur Window.

[31] The sequential appearance and timing of the non-metamorphosed Inner Lesser Himalayan cover and metamorphosed Inner Lesser Himalaya (LHCS) is consistent with our tectonic reconstruction. Prior to exhumation of the ILH metamorphic rocks, the part of the Inner Lesser Himalaya exhumed would have been that subducted beneath the MCT only to shallow depths, probably a sedimentary cover to the deeper Jutogh schists and Wangtu gneisses, such as the Rampur quartzites. This is reflected in the earlier occurrence of quartzite conglomerate clasts with Inner Lesser Himalayan  $\varepsilon_{\text{Nd}}$  (500) signatures. Assuming Rampur quartzites of chlorite grade (closure temperature ca 300–350°C) exposed at 9 Ma, Jutogh and Wangtu LHCS cooling through 625°C at  $\sim 7$  kbar at 11 Ma [Caddick *et al.*, 2007], an exhumation rate of 3 mm/yr [Thiede *et al.*, 2009], it would take 4 Myr for the additional 12 km of material to be exhumed subsequent to Rampur Formation exposure at 9 Ma. This would place LHCS exposure at 5 Ma, consistent with the first substantial appearance of its detritus observed in the sediment record at 5–6 Ma. Major exhumation of the LHCS is also reflected in markedly decreased contribution from the Haimanta “cover” from this time.

[32] After 6 Ma, erosion from the Inner Lesser Himalaya was sufficient to dominate the sedimentary signal as shown by  $\varepsilon_{\text{Nd}}$  bulk rock data now with Lesser Himalayan values and mica Ar-Ar ages showing that the Higher Himalayan and Haimanta material was entirely cut out. The spatially restricted nature of this drastic provenance change (the coeval sample from Haripur outside the reentrant continues to show Higher Himalayan input) is consistent with our interpretation of a localized source region, the Rampur Window, subjected to tectonic exhumation during that period.

## 6. Summary and Further Implications

[33] The exhumation rate of the Higher Himalaya decreased markedly shortly before 16 Ma, after which the Higher Himalaya continued to exhume to deeper metamorphic levels but at much slower rates and thrusting transferred into the footwall of the MCT. The Lesser Himalaya lies in the footwall of the MCT, but first to be exhumed was its overlying Haimanta cover, which contributed a substantial input to the sedimentary record from 17 Ma [White *et al.*, 2002]. Nonmetamorphosed Lesser Himalaya was exhumed to surface by 9 Ma. Major exhumation of the Lesser Himalaya, including exhumation to surface of the Lesser Himalayan Crystalline Series, occurred at 6 Ma causing major disruption to river drainage patterns.

[34] Our interpretations agree in part with those of previous workers [Brozovic and Burbank, 2000; Meigs *et al.*, 1995] who recognized Lesser Himalayan material in the conglomerates younger than 9 Ma. However, contrary to previous work, we do not infer that these conglomerates date movement along the Main Boundary Thrust. The MBT is the most southerly of thrusts exhuming the Lesser Himalaya, and more northerly thrusts, for example the Munsiri Thrust as exposed in the Rampur Window, likely exhumed Lesser Himalayan material earlier. Such tectonics have already been proposed in Nepal, where DeCelles *et al.* [1998] document exhumation of the Lesser Himalayan duplex, prior to MBT motion.

[35] Our data can also be compared with a recent numerical model which explains a number of features of the orogen, in particular exhumation of the Higher Himalaya, by extrusion of a low velocity lower midcrust by channel flow [Beaumont *et al.*, 2001]. The timing of first appearance at surface of rocks of progressively increasing metamorphic grade is predicted by the model [Jamieson *et al.*, 2004], and can be tested by documenting the timing of first appearance of specific metamorphic minerals in the erosional record, assuming rapid transport from source to sink. In the model, greenschist facies (garnet present) is predicted to appear at surface at ca 25 Ma, becoming the dominant material being eroded by 20 Ma. At this time amphibolite material (staurolite and possibly kyanite) should first appear at surface, contributing significantly to the detritus by ca 15 Ma. At 15 Ma migmatite, perhaps containing kyanite and/or sillimanite, is predicted to first appear at surface, contributing significantly to material being eroded by 10 Ma. Our data from the Indian foreland basin, encompassing new data from the Siwalik Group and previously published data from the older Dharamsala, Dagshai and Kasauli Formation are consistent with these model predictions. Subgreenschist facies were being eroded into the basin in NW India during deposition of the Dagshai Formation, with significant erosion of garnet-bearing lithologies around ca 20 Ma (in the Kasauli and Lower Dharamsala Formations) [Najman and Garzanti, 2000; White *et al.*, 2002]. Rare staurolite is sporadically present at 20 Ma [White *et al.*, 2002], and kyanite at 13 Ma (this study). However, the appearance of sillimanite at 8 Ma is later than model predictions.

[36] In order for our interpretations to be robust, we need to know the degree to which variations in the sediment record reflect changes in drainage rather than tectonics. In an actively prograding fold-thrust belt, changes in tectonics and drainage patterns are likely to be interlinked. The occurrence of nonmetamorphosed Lesser Himalaya in the sedimentary record at 9 Ma, and LHCS detritus at 6 Ma is indisputable evidence that these units had exhumed to surface by this time, but still earlier exhumation of these units, with their products of erosion diverted elsewhere, is a concept that cannot be ruled out. In the present study, the good temporal correlation between the tectonic events dated from bedrock geology [Caddick *et al.*, 2007; Chambers *et al.*, 2009; Thiede *et al.*, 2005; Vannay *et al.*, 2004] and the coeval response in the sediment record, suggests a tectonic cause for the changes observed. In addition, our data

(although not always interpretation) are similar to those obtained from analogous sedimentary studies many kilometers along strike in Nepal [Bernet *et al.*, 2006; DeCelles *et al.*, 1998; Huyghe *et al.*, 2001; Robinson *et al.*, 2001; Szulc *et al.*, 2006] and our proposed timing for major thrusting of the Lesser Himalaya is consistent with the timing proposed for this event along strike in Nepal [Robinson *et al.*, 2006] and with an increase in sediment

accumulation rates in the foreland basin at 11 Ma from Pakistan to western Nepal, interpreted as the result of increased subsidence due to loading by the major new thrust system of the Lesser Himalaya [Burbank *et al.*, 1996; Ojha *et al.*, 2008].

[37] **Acknowledgments.** To Ewan Laws and Dodi Najman for field assistance and to Tom Argles, Mark Caddick, Jen Chambers, and Rasmus Thiede for discussion on interpretation of the data.

## References

- Ahmad, T., N. Harris, M. Bickle, H. Chapman, J. Bunbury, and C. Prince (2000), Isotopic constraints on the structural relationships between the Lesser Himalayan Series and the High Himalayan Crystalline Series, Garhwal Himalaya, *Geol. Soc. Am. Bull.*, *112*(3), 467–477, doi:10.1130/0016-7606(2000)112<0467:ICOTSR>2.3.CO;2.
- Amidon, W. H., D. W. Burbank, and G. E. Gehrels (2005), U-Pb zircon ages as a sediment mixing tracer in the Nepal Himalaya, *Earth Planet. Sci. Lett.*, *235*(1–2), 244–260, doi:10.1016/j.epsl.2005.03.019.
- Beaumont, C., R. A. Jamieson, M. H. Nguyen, and B. Lee (2001), Himalayan tectonics explained by extrusion of a low-viscosity crustal channel coupled to focused surface denudation, *Nature*, *414*(6865), 738–742, doi:10.1038/414738a.
- Bernet, M., M. Zattin, J. I. Garver, M. T. Brandon, and J. A. Vance (2001), Steady-state exhumation of the European Alps, *Geology*, *29*(1), 35–38, doi:10.1130/0091-7613(2001)029<0035:SSEOTE>2.0.CO;2.
- Bernet, M., P. van der Beek, R. P. K. Huyghe, J. L. Mugnier, E. Labrin, and A. Szulc (2006), Miocene to Recent exhumation of the central Himalaya determined from combined detrital zircon fission-track and U/Pb analysis of Siwalik sediments, western Nepal, *Basin Res.*, *18*(4), 393–412, doi:10.1111/j.1365-2117.2006.00303.x.
- Bickle, M. J., N. B. W. Harris, J. M. Bunbury, H. J. Chapman, I. J. Fairchild, and T. Ahmad (2001), Controls on the Sr-87/Sr-86 ratio of carbonates in the Garhwal Himalaya, headwaters of the Ganges, *J. Geol.*, *109*(6), 737–753, doi:10.1086/323192.
- Brozovic, N., and D. W. Burbank (2000), Dynamic fluvial systems and gravel progradation in the Himalayan foreland, *Geol. Soc. Am. Bull.*, *112*(3), 394–412, doi:10.1130/0016-7606(2000)112<0394:DFSAGP>2.3.CO;2.
- Burbank, D. W., R. A. Beck, and T. Mulder (1996), The Himalayan foreland basin, in *The Tectonic Evolution of Asia*, edited by A. Yin and T. M. Harrison, pp. 149–188, Cambridge Univ. Press, Cambridge, U. K.
- Caddick, M. J., M. J. Bickle, T. J. B. Holland, M. B. W. Harris, M. S. A. Horstwood, R. R. Parrish, T. Argles, and T. Ahmad (2007), Burial and exhumation history of a Lesser Himalayan schist: Recording the formation of an inverted metamorphic sequence in NW India, *Earth Planet. Sci. Lett.*, *264*, 375–390, doi:10.1016/j.epsl.2007.09.011.
- Chambers, J., M. J. Caddick, T. Argles, M. Horstwood, S. Sherlock, N. Harris, R. Parrish, and T. Ahmad (2009), Empirical constraints on extrusion mechanisms from the upper margin of an exhumed high-grade orogenic core, Sutlej Valley, NW India, *Tectonophysics*, doi:10.1016/j.tecto.2008.10.013, in press.
- DeCelles, P. G., G. E. Gehrels, J. Quade, T. P. Ojha, P. A. Kapp, and B. N. Upreti (1998), Neogene foreland basin deposits, erosional unroofing, and the kinematic history of the Himalayan fold-thrust belt, western Nepal, *Geol. Soc. Am. Bull.*, *110*(1), 2–21, doi:10.1130/0016-7606(1998)110<0002:NFBDEU>2.3.CO;2.
- de Sigoyer, J., V. Chavagnac, J. Blichert-Toft, I. M. Villa, B. Luais, S. Guillot, M. Cosca, and G. Mascle (2000), Dating the Indian continental subduction and collisional thickening in the northwest Himalaya: Multichronology of the Tso Moriri eclogites, *Geology*, *28*(6), 487–490, doi:10.1130/0091-7613(2000)28<487:DTICSA>2.0.CO;2.
- English, N. B., J. Quade, P. G. DeCelles, and C. N. Garzione (2000), Geologic control of Sr and major element chemistry in Himalayan Rivers, Nepal, *Geochim. Cosmochim. Acta*, *64*(15), 2549–2566, doi:10.1016/S0016-7037(00)00379-3.
- France-Lanord, C., L. Derry, and A. Michard (1993), Evolution of the Himalaya since Miocene time: Isotopic and sedimentological evidence from the Bengal Fan, in *Himalayan Tectonics*, edited by P. J. Treloar and M. P. Searle, *Geol. Soc. Spec. Publ.*, *74*, 603–622.
- Frank, W., B. Grasemann, P. Guntli, and C. Miller (1995), Geological map of the Kishitwar-Chambakulu region (NW Himalayas, India), *Jahrb. Geol. Bundesanst.*, *138*(2), 299–308.
- Gaetani, M., and E. Garzanti (1991), Multicyclic history of the northern India continental-margin (northwestern Himalaya), *AAPG Bull.*, *75*(9), 1427–1446.
- Galy, A., C. France-Lanord, and L. A. Derry (1999), The strontium isotopic budget of Himalayan rivers in Nepal and Bangladesh, *Geochim. Cosmochim. Acta*, *63*(13–14), 1905–1925, doi:10.1016/S0016-7037(99)00081-2.
- Garzanti, E., A. Baud, and G. Mascle (1987), Sedimentary record of the northward flight of India and its collision with Eurasia (Ladakh Himalaya, India), *Geodin. Acta*, *1*(4–5), 297–312.
- Huyghe, P., A. Galy, J. L. Mugnier, and C. France-Lanord (2001), Propagation of the thrust system and erosion in the Lesser Himalaya: Geochemical and sedimentological evidence, *Geology*, *29*(11), 1007–1010, doi:10.1130/0091-7613(2001)029<1007:POTTSA>2.0.CO;2.
- Ingersoll, R. V., T. F. Bullard, R. L. Ford, J. P. Grimm, J. D. Pickle, and S. W. Sares (1984), The effect of grain-size on detrital modes: A test of the Gazzi-Dickinson point-counting method, *J. Sediment. Petrol.*, *54*, 103–116.
- Jamieson, R. A., C. Beaumont, S. Medvedev, and M. H. Nguyen (2004), Crustal channel flows: 2. Numerical models with implications for metamorphism in the Himalayan-Tibetan orogen, *J. Geophys. Res.*, *109*, B06407, doi:10.1029/2003JB002811.
- Mange, M. A., and H. F. Maurer (1992), *Heavy Minerals in Colour*, 147 pp. Chapman and Hall, London.
- Meigs, A. J., D. W. Burbank, and R. A. Beck (1995), Middle-late Miocene (>10 Ma) Formation of the Main Boundary Thrust in the western Himalaya, *Geology*, *23*(5), 423–426, doi:10.1130/0091-7613(1995)023<0423:MLMMFO>2.3.CO;2.
- Miller, C., U. Klotzli, W. Frank, M. Thoni, and B. Grasemann (2000), Proterozoic crustal evolution in the NW Himalaya (India) as recorded by circa 1.80 Ga mafic and 1.84 Ga granitic magmatism, *Precambrian Res.*, *103*, 191–206, doi:10.1016/S0301-9268(00)00091-7.
- Miller, C., M. Thoni, W. Frank, B. Grasemann, U. Klotzli, P. Guntli, and E. Draganits (2001), The early Palaeozoic magmatic event in the Northwest Himalaya, India: Source, tectonic setting and age of emplacement, *Geol. Mag.*, *138*, 237–251, doi:10.1017/S0016756801005283.
- Najman, Y., and E. Garzanti (2000), Reconstructing early Himalayan tectonic evolution and paleogeography from Tertiary foreland basin sedimentary rocks, northern India, *Geol. Soc. Am. Bull.*, *112*(3), 435–449, doi:10.1130/0016-7606(2000)112<0435:REHTEA>2.3.CO;2.
- Najman, Y., E. Garzanti, M. Pringle, M. Bickle, J. Stix, and I. Khan (2003), Early Mid Miocene palaeodrainage and tectonics in the Pakistan Himalaya, *Geol. Soc. Am. Bull.*, *115*, 1265–1277, doi:10.1130/B25165.1.
- Ojha, T., R. Butler, P. DeCelles, and J. Quade (2008), Magnetic polarity stratigraphy of the Neogene foreland basin deposits of Nepal, *Basin Res.*, *112*(3), 424–434, doi:10.1130/0016-7606(2000)112<424:MPSTOTN>2.0.CO;2.
- Pierson-Wickmann, A.-C., L. Reisberg, and C. France-Lanord (2000), The Os isotopic composition of Himalayan river bedloads and bedrocks: Importance of black shales, *Earth Planet. Sci. Lett.*, *176*, 203–218, doi:10.1016/S0012-821X(00)00003-0.
- Quade, J., L. Roe, P. G. DeCelles, and T. P. Ojha (1997), The late Neogene <sup>87</sup>Sr/<sup>86</sup>Sr record of lowland Himalayan rivers, *Science*, *276*(5320), 1828–1831, doi:10.1126/science.276.5320.1828.
- Quade, J., N. English, and P. G. DeCelles (2003), Silicate versus carbonate weathering in the Himalaya: A comparison of the Arun and Seti River watersheds, *Chem. Geol.*, *202*(3–4), 275–296, doi:10.1016/j.chemgeo.2002.05.002.
- Richards, A., T. W. A. Argles, N. B. W. Harris, R. Parrish, T. Ahmad, F. Darbeyshire, and E. Draganits (2005), Himalayan architecture constrained by isotopic tracers from clastic sediments, *Earth Planet. Sci. Lett.*, *236*, 773–796, doi:10.1016/j.epsl.2005.05.034.
- Robinson, D. M., P. G. DeCelles, P. J. Patchett, and C. N. Garzione (2001), The kinematic evolution of the Nepalese Himalaya interpreted from Nd isotopes, *Earth Planet. Sci. Lett.*, *192*(4), 507–521, doi:10.1016/S0012-821X(01)00451-4.
- Robinson, D. M., P. G. DeCelles, and P. Copeland (2006), Tectonic evolution of the Himalayan thrust belt in western Nepal: Implications for channel flow models, *Geol. Soc. Am. Bull.*, *118*(7–8), 865–885, doi:10.1130/B25911.1.
- Sangode, S. J., R. Kumar, and S. K. Ghosh (1996), Magnetic polarity stratigraphy of the Siwalik sequence at Haripur area (HP) NW India, *J. Geol. Soc. India*, *47*, 683–704.
- Searle, M., R. I. Corfield, B. Stephenson, and J. McCarron (1997), Structure of the North Indian continental margin in the Ladakh-Zaskar Himalayas: Implications for the timing of obduction of the Spontang ophiolite, India-Asia collision and deformation events in the Himalaya, *Geol. Mag.*, *134*(3), 297–316, doi:10.1017/S0016756897006857.
- Steck, A. (2003), Geology of the NW Indian Himalaya, *Eclogae Geol. Helv.*, *96*(2), 147–196.
- Stephenson, B. J., M. P. Searle, D. J. Waters, and D. C. Rex (2001), Structure of the Main Central Thrust

- zone and extrusion of the High Himalayan deep crustal wedge, Kishitwar-Zanskar Himalaya, *J. Geol. Soc.*, *158*, 637–652.
- Szulec, A. G., et al. (2006), Tectonic evolution of the Himalaya constrained by a detrital investigation of three Siwalik foreland basin deposits, SW Nepal, *Basin Res.*, *18*, 375–391, doi:10.1111/j.1365-2117.2006.00307.x.
- Thiede, R. C., B. Bookhagen, J. R. Arrowsmith, E. R. Sobel, and M. R. Strecker (2004), Climate control on rapid exhumation along the southern Himalayan front, *Earth Planet. Sci. Lett.*, *222*, 791–806, doi:10.1016/j.epsl.2004.03.015.
- Thiede, R. C., J. R. Arrowsmith, B. Bookhagen, M. O. McWilliams, E. R. Sobel, and M. R. Strecker (2005), From tectonically to erosionally controlled development of the Himalayan orogen, *Geology*, *33*(8), 689–692, doi:10.1130/G21483.1.
- Thiede, R. C., T. A. Ehlers, B. Bookhagen, and M. R. Strecker (2009), Erosional variability along the northwest Himalaya, *J. Geophys. Res.*, *114*, F01015, doi:10.1029/2008JF001010.
- Vance, D., and N. Harris (1999), Timing of prograde metamorphism in the Zanskar Himalaya, *Geology*, *27*(5), 395–398, doi:10.1130/0091-7613(1999)027<0395:TOPMIT>2.3.CO;2.
- Vannay, J.-C., B. Grasemann, M. Rahn, W. Frank, A. Carter, V. Baudraz, and M. Cosca (2004), Miocene to Holocene exhumation of metamorphic crustal wedges in the NW Himalaya: Evidence for tectonic extrusion coupled to fluvial erosion, *Tectonics*, *23*, TC1014, doi:10.1029/2002TC001429.
- White, N. M., R. R. Parrish, M. J. Bickle, Y. M. R. Najman, D. Burbank, and A. Maitani (2001), Metamorphism and exhumation of the NW Himalaya constrained by U-Th-Pb analyses of detrital monazite grains from early foreland basin sediments, *J. Geol. Soc.*, *158*, 625–635.
- White, N. M., M. Pringle, E. Garzanti, M. Bickle, Y. Najman, H. Chapman, and P. Friend (2002), Constraints on the exhumation and erosion of the High Himalayan Slab, NW India, from foreland basin deposits, *Earth Planet. Sci. Lett.*, *195*(1–2), 29–44, doi:10.1016/S0012-821X(01)00565-9.
- Zuffa, G. G. (1985), Optical analyses of arenites: Influence of methodology on compositional results, in *Provenance of Arenites, NATO Adv. Stud. Inst.*, vol. *148*, edited by G. G. Zuffa, pp. 165–189, D. Reidel, Dordrecht, Netherlands.
- S. Ando and E. Garzanti, Dipartimento di Geologiche e Geotechnologie, Università Milano-Bicocca, Piazza della Scienza 4, I-20126 Milano, Italy.
- D. Barfod and M. Pringle, SUERC, Rankine Avenue, Scottish Enterprise Technology Park, East Kilbride G75 0QF, UK.
- M. Bickle, Department of Earth Science, University of Cambridge, Downing St., Cambridge CB2 3EQ, UK.
- N. Brozovic, Department of Agricultural and Consumer Economics, University of Illinois, Mumford Hall, 1301 West Gregory Drive, Urbana, IL, 61801-3605, USA.
- D. Burbank, Department of Earth Sciences, University of California, 1006 Webb Hall, MC9630, Santa Barbara, CA 93106-9630, USA.
- Y. Najman, Lancaster Environment Centre, Lancaster University, Lancaster LA1 4YQ, UK. (y.najman@lancaster.ac.uk)